Journal of Geoscience and Environment Protection, 2026, 14(9), 96-116
https://www.scirp.org/journal/gep
ISSN Online: 2327-4344
ISSN Print: 2327-4336

Petrographic and Geochemical Characterization of the Kibalian Formations in the Lassa Area (Haut-Uélé Province, Democratic Republic of the Congo): Implications for Hydrothermal Alteration and Mineral Exploration

Blaise Mutombo Kabulu[1*], Richard Logro Sapa[1], Divine Biaya Tshiala[2], Herman Sadimoke Ibingo[3], Jean-Paul Bakajika Kabongo[1], Jean-Luc Albini Tshupa[2], Junior Lele Mambwiya[1], Joseph Lelo Nkenge[1], Adalbert Jules Makutu Ma Ngwayaya[2], Giresse Kabemba Kalonji[1]

[1]Geological and Mining Research Center (CRGM), Ministry of ESURSI, Kinshasa, Democratic Republic of the Congo
[2]Faculty of Science and Technology, University of Kinshasa, Kinshasa, Democratic Republic of the Congo
[3]Faculty of Sciences, University of Haut-Uélé, Isiro, Democratic Republic of the Congo
Email: *blaisexavierkabulu@gmail.com

How to cite this paper: Kabulu, B. M., Sapa, R. L., Tshiala, D. B., Ibingo, H. S., Kabongo, J.-P. B., Tshupa, J.-L. A., Mambwiya, J. L., Nkenge, J. L., Ngwayaya, A. J. M. M., & Kalonji, G. K. (2026). Petrographic and Geochemical Characterization of the Kibalian Formations in the Lassa Area (Haut-Uélé Province, Democratic Republic of the Congo): Implications for Hydrothermal Alteration and Mineral Exploration. *Journal of Geoscience and Environment Protection, 14,* 96-116.
https://doi.org/10.4236/gep.2026.149007

Received: July 7, 2026
Accepted: September 18, 2026
Published: September 21, 2026

Abstract

This study investigates the petrographic, geochemical, and metallogenic characteristics of the Kibalian formations in the Lassa area of Haut-Uélé Province, northeastern Democratic Republic of the Congo. The aim is to improve geological knowledge and assess the mineral potential of this poorly documented region. Geological field investigations were conducted at thirteen sampling stations, where representative rock samples were collected. Three samples were selected for petrographic analysis by thin-section microscopy, and three representative samples were analysed by X-ray fluorescence (XRF) to determine their major-oxide and trace-element compositions. Petrographic investigations identified three principal lithological units: dolerite, granite, and banded iron formation. Geochemical analyses revealed marked compositional differences among these lithologies. The quartz-vein sample has a high SiO_2 content and elevated Cr, Cu, and Zn concentrations, whereas the BIF samples show iron enrichment and geochemical signatures consistent with hydrothermal alteration. Reflected-light microscopy confirmed the occurrence of pyrite within the quartz vein. Together, the petrographic, geochemical, and metallographic observations indicate that hydrothermal-fluid circulation played an important role in the evolution of the study area and suggest favourable conditions for hydrothermal mineralization. Although no direct gold analyses were performed, the results identify the Lassa area as a promising target for further mineral-exploration studies.

Keywords

Kibalian Greenstone Belt, Petrography, Geochemistry, Hydrothermal Alteration, Mineral Exploration

1. Introduction

The northeastern Democratic Republic of the Congo (DRC) contains some of the most prospective Precambrian terranes in Central Africa and is renowned for abundant mineral resources, particularly gold and iron. Among these geological domains, the Kibalian Supergroup has attracted considerable scientific and economic interest because it comprises Archean volcano-sedimentary sequences intruded by granitoids and mafic rocks, forming a favourable geological environment for hydrothermal mineralization. Despite its economic importance, several sectors of the Kibalian belt, including the Lassa area in Haut-Uélé Province, remain insufficiently documented from petrographic and geochemical perspectives. Further investigation is therefore required to improve understanding of these formations and assess their mineral potential.

The Geological Commission of the former Belgian Ministry of Colonies formally introduced the Kibalian Group to describe rock units that had previously been assigned to the Itabirite System, the Ferruginous Series, or the Algonkian succession (de Dorlodot & Mathieu, 1928, 1929, 1931). Subsequently, Cahen and Lepersonne (1956, 1967) described the Kibalian succession as a heterogeneous assemblage of sericite-chlorite schist, biotite schist, quartzites, conglomerates, carbonate rocks, volcanic rocks, tuffs, itabirites, and granitoids. These lithological associations record a complex geological evolution involving magmatism, sedimentation, deformation, and regional metamorphism during the Archean and Paleoproterozoic.

Previous investigations have shown that the Kibalian formations underwent intense regional metamorphism and deformation, making field identification of the original lithologies particularly challenging (Duhoux, 1950). Amphibolite-facies metamorphism, accompanied by strong foliation and hydrothermal alteration, has significantly modified the primary mineralogical and textural characteristics of these rocks (Cahen & Lepersonne, 1967). Nevertheless, remnants of volcanic, plutonic, and chemical sedimentary rocks are preserved and provide valuable in-formation on the geological evolution of the Kibalian greenstone belts and their associated mineralization.

The Lassa area forms part of this geological framework and is characterized by granitoids, doleritic intrusions, quartz veins, and banded iron formations (BIFs), all commonly associated with hydrothermal processes in Precambrian greenstone belts. Quartz veins containing sulphide minerals and hematite-rich iron formations are favourable geological indicators of orogenic gold mineralization and therefore warrant detailed petrographic and geochemical investigation.

This study aims to characterize the principal lithological units exposed in the Lassa area through integrated field observations, petrographic investigations, X-ray fluorescence (XRF) geochemical analyses, and metallographic observations. The objectives are to: 1) identify the principal lithofacies; 2) determine their mineralogical and geochemical characteristics; 3) evaluate the effects of hydrothermal alteration; and 4) discuss the implications of these results for the metallogenic potential of the Lassa area within the Kibalian greenstone belt.

2. Materials and Methods

2.1. Study Area

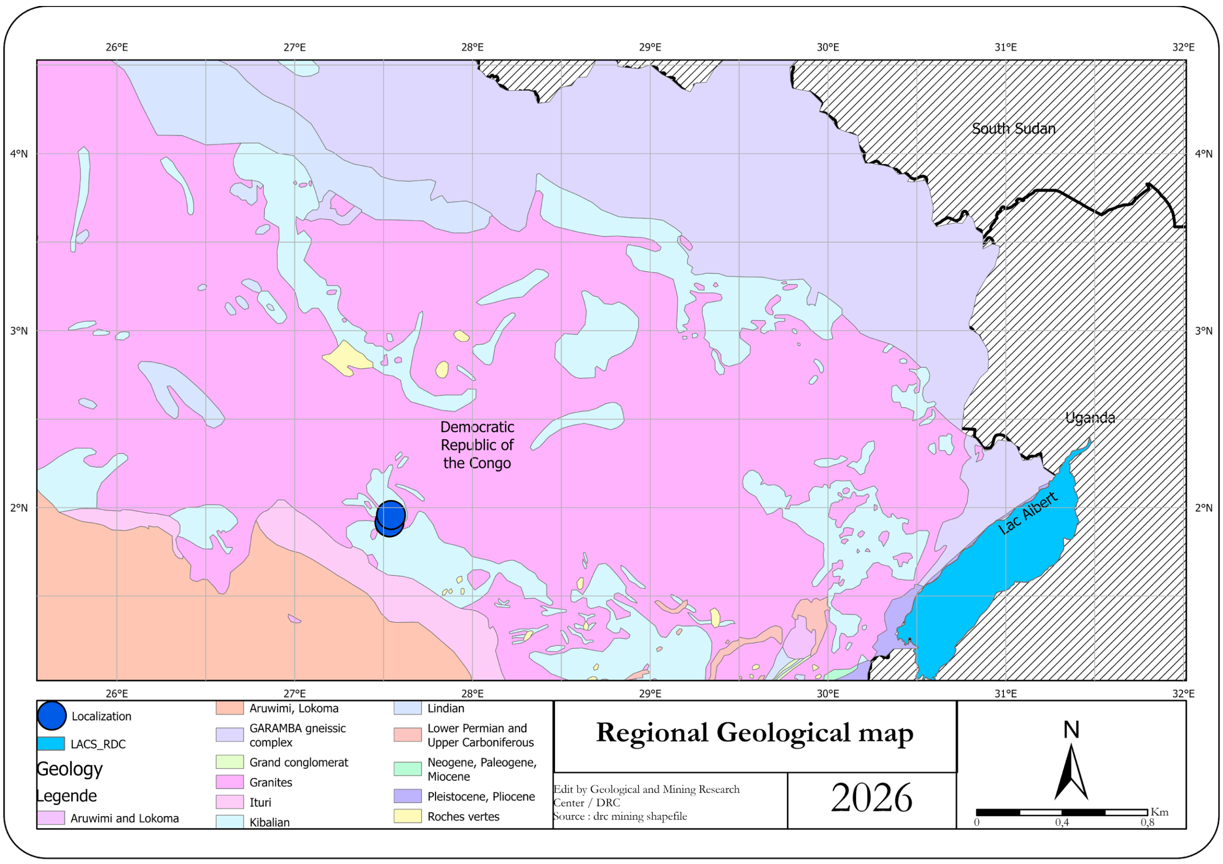

Figure 1. Geological map showing the Upper Zaire granitoid massif, the associated Kibalian greenstone belts, and cratonic blocks.

The study area is located in the Lassa region of Wamba Territory, Haut-Uélé Province, northeastern Democratic Republic of the Congo, approximately 130 km south of Isiro (Figure 1). Geographically, the area lies between longitudes 27˚32'00" E and 27˚32'30" E and latitudes 1˚55'00" N and 1˚57'30" N (Figure 2). It belongs to the Kibalian greenstone belt, which is enclosed within the Upper Zaire granitoid massif and forms part of the northeastern Congo Craton (Lavreau, 1982; Lepersonne, 1974).

The region has a humid tropical climate, abundant rainfall throughout the year, and dense equatorial rainforest. This vegetation substantially limits bedrock exposure, such that geological observations are mainly possible along river channels, erosion surfaces, road cuts, and artisanal-mining excavations.

The study area is accessible through a network of secondary roads connecting Isiro with Wamba Territory and surrounding villages. Artisanal-mining activities have locally improved rock exposure, facilitating lithological mapping and sampling.

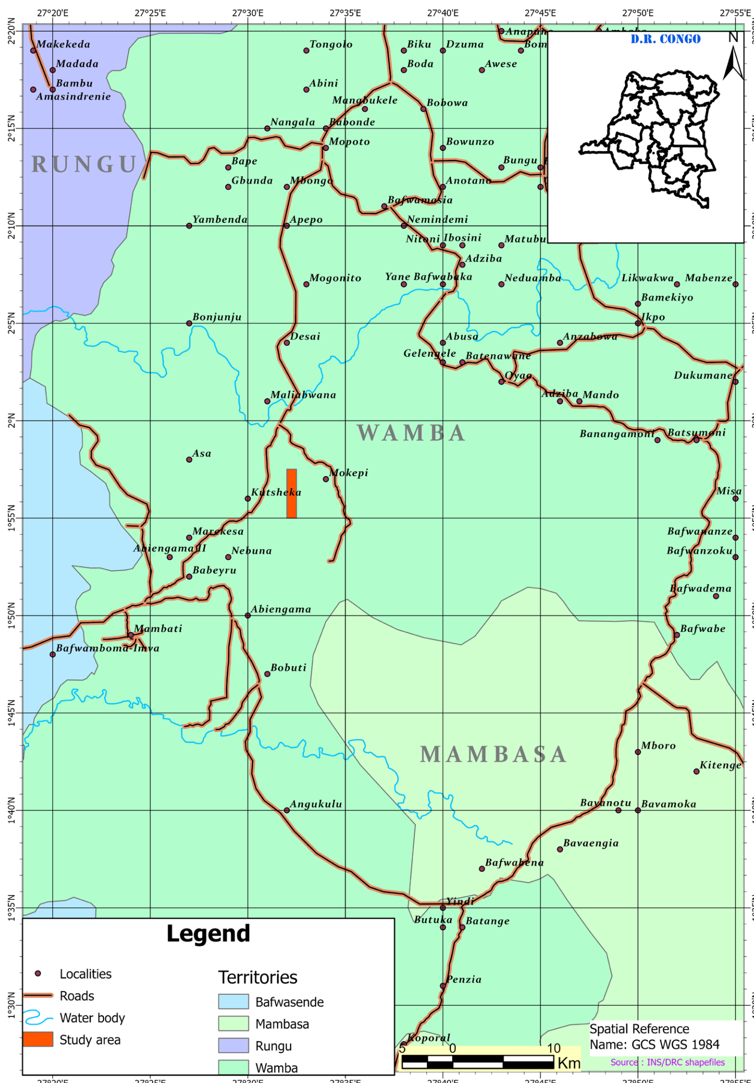

Figure 2. Location map of the study area in Haut-Uélé Province.

2.2. Geological Setting

The Lassa area belongs to the Paleoproterozoic Kibalian greenstone belt, one of the principal greenstone belts of the northeastern Congo Craton. The Kibalian belt consists of metavolcanic and metasedimentary sequences intruded by granitoid bodies during the Eburnean orogenic event. These units record a complex tectono-metamorphic evolution involving crustal accretion, deformation, metamorphism, and hydrothermal activity (Cahen et al., 1984). This framework is consistent with the regional geological map of Zaire (Geological Survey of Zaire, 1974) and the lithostratigraphic evolution of northern DRC (Verbeek, 1970).

In the study area, the lithological assemblage includes granitoids, doleritic intrusions, metavolcanic rocks, banded iron formations, quartz veins, and locally silicified rocks. Quartz veins occur as fracture fillings and are commonly associated with iron-oxide alteration. Granitoids constitute the dominant basement rocks, whereas BIF and metavolcanic units occur as discontinuous bands within the greenstone sequence.

Structurally, the area is affected by brittle and ductile deformation expressed by faults, fractures, foliations, and quartz veins trending predominantly NE-SW and NW-SE. These structures acted as preferential pathways for hydrothermal fluids responsible for silicification, hematitization, chloritization, and iron enrichment. Such hydrothermal-alteration features are commonly associated with mineralized systems throughout the Kibalian greenstone belt.

Kibalian rocks are oriented mainly NW-SE to NNW-SSE and N-S, with subordinate NE-SW and E-W trends in the granitic basement, the orthogneissic complex, and the Upper Kibalian, particularly within the itabirite beds. These Upper Kibalian formations have undergone intensive folding (Lavreau & Ledent, 1975).

These rocks can be grouped into two main sets: an elongated assemblage of metamorphic rocks surrounded by various granitic rocks, including a western Upper Kibalian metasedimentary facies (Ks) and an eastern Lower Kibalian metavolcanic facies (Ki). The two sets are separated by a major unconformity; consequently, the distinction between the Lower and Upper Kibalian is justified, at least locally (Lavreau, 1982). The regional geological framework of the study area is illustrated in **Figure 3**.

The tectonic control on relief is particularly evident along the upper Bomokandi River near Rungu and in the Moto mining region, where itabirite bands appear to provide useful stratigraphic markers.

In the eastern Moto area (Makoro region), the itabirites form N-S-oriented bands. Similar trends occur in the western area between Telekudu-Moku in the south and Motobi-VKV in the north, and farther west toward Tora. In the central sector around Doko-Durba, however, the dominant trends are approximately E-W (Mbo et al., 2024). These characteristics are comparable to those reported from the Kilo-Moto mining district (Legraye, 1940).

A broad basin-like structure is also expressed by the itabirites. Two tectonic domains can be distinguished: the Dungu domain, which has a general ENE trend, and the Niangara domain, which has a NW trend.

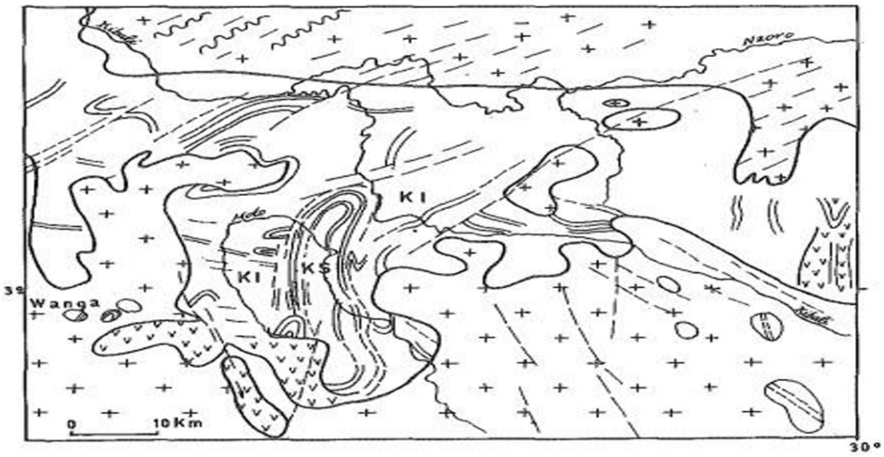

Figure 3. Geological and structural sketch of the central part of the Kibalian belt at Moto (belt boundary after Lepersonne, 1974). Ki = Lower Kibalian (schistose and massive facies); Ks = Upper Kibalian (quartzite and itabirite levels); + = granitoid massif. The West Nile Gneissic Complex occurs to the north (Lavreau, 1982).

2.3. Sampling and Analytical Methods

Field investigations were conducted at thirteen observation and sampling stations to characterize lithological units and identify representative sampling sites. Geological mapping included observations of lithology, structural features, alteration patterns, and quartz-vein distribution. Representative rock samples were collected from fresh outcrops and artisanal-mining excavations to minimize the effects of weathering. Three representative specimens (BD01, BD02, and BD06) were selected for petrographic analysis, whereas three samples (BD05, BD06, and BD01b) were selected for whole-rock geochemical and metallographic analyses.

Petrographic analyses were conducted on polished thin sections using a polarizing optical microscope to determine mineralogical composition, textures, and alteration features.

Whole-rock geochemical analyses were performed by X-ray fluorescence at CREN-K (Centre de Recherche en Énergie et Sciences Nucléaires de Kinshasa), DRC. Major elements were determined and reported as oxide weight percentages (wt.%), whereas trace elements were expressed in parts per million (ppm). The results were processed using conventional geochemical classification diagrams and elemental ratios to characterize the lithologies and evaluate hydrothermal-alteration processes.

3. Results

3.1. Field Observations

The field survey enabled the preparation of a location map for the observation and sampling stations, identified by the prefix BD (**Figure 4**). The geographical coordinates of the principal observation and sampling stations are summarized in **Table 1**.

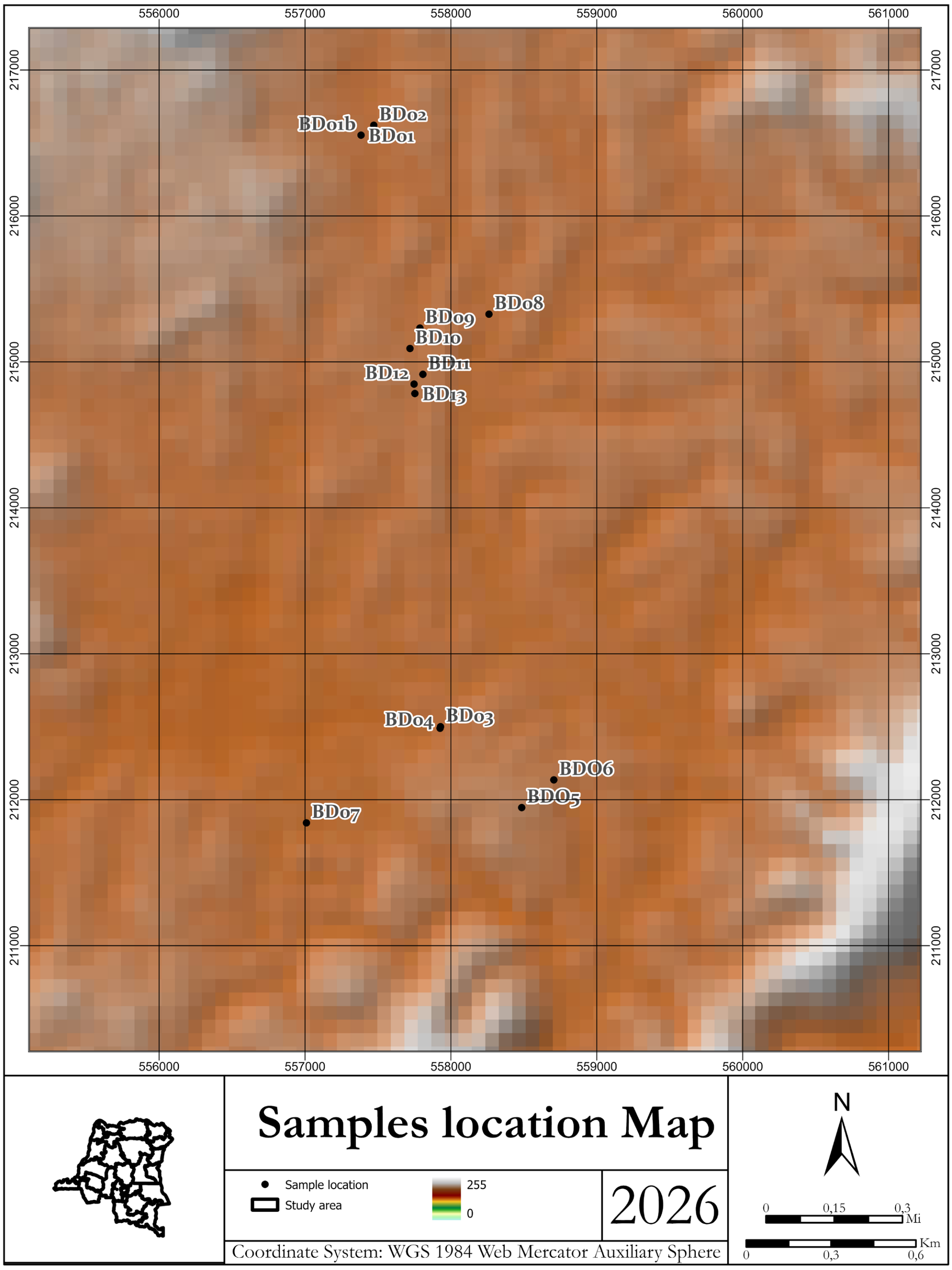

Figure 4. Map showing the locations of observation and sampling stations.

Field investigations showed that the study area is dominated by granitoids, banded iron formations, doleritic dykes, quartz veins, and locally silicified rocks. Outcrops are generally scarce because of dense equatorial vegetation and a thick lateritic weathering profile. Most geological observations were therefore made along river channels, in artisanal-mining pits, and at road cuts.

The granitoids are generally coarse-grained and locally affected by fracturing and hydrothermal alteration. Quartz veins occur as isolated veins or vein networks cutting across the host rocks. Their thickness ranges from a few centimetres to several metres, and they commonly display massive, milky-white, or translucent textures. Iron-oxide staining is frequently observed along fractures and vein margins.

The BIFs occur as discontinuous bands composed predominantly of alternating silica-rich and iron-rich layers. At several localities, these rocks exhibit intense silicification and hematitization, indicating substantial hydrothermal overprinting. Doleritic dykes cross-cut both the granitoids and the metavolcanic sequence, confirming that they represent younger intrusive events.

Hydrothermal alteration is widespread throughout the study area and is mainly expressed as silicification, iron-oxide enrichment, chloritization, and local sericitization. These alteration features are particularly developed around quartz veins and fracture zones, suggesting that structural discontinuities controlled fluid circulation during hydrothermal events.

Table 1. Coordinates of the principal observation and sampling stations in the Lassa region.

Observation Station	Altitude (m)			Description
	Easting	Northing	Altitude (m)	
BD01	557,384	216,554	667	Medium-grained, grey-green rock with a massive appearance, containing feldspar and quartz. Iron sulphides are also present. The rock is cut by a 50-cm-thick quartz vein (N235˚/78˚ NW).
BD01b	557,384	216,554	668	Milky-white quartz vein containing millimetre- to centimetre-scale, subrounded to elliptical nodules rich in bright-yellow iron sulphide (pyrite).
BD02	557,471	216,621	669	Massive rock with medium grain size, grey in color with minerals including: quartz, muscovite, orthoclase, biotite.
BD03	557,929	212,501	667	Medium-sized rock, grey-green in color, with a massive appearance, containing feldspar and peridots as minerals. Arsenic is present.
BD04	557,926	212,490	671	Medium-sized rock, grey-green in color, with a massive appearance and containing the following minerals: feldspar, peridots and arsenic.
BD05	558,485	211,946	696	Massive red-black rock with foliation. Minerals: Magnetite, hematite and quartz. **Folio: N275/42**
BD06	558,705	212,136	692	Massive brown rock with foliation. Minerals: Magnetite, hematite and quartz. **Folio: N274/32**
BD07	557,010	211,842	687	Medium-sized rock, grey-green in color, with a massive appearance and containing the following minerals: feldspar, peridots.

Continued

BD08	558,261	215,327	664	Medium grain size rock, grey-green in color with a massive appearance, containing the following minerals: feldspar, peridots.
BD09	557,787	215,232	677	Medium-sized rock, grey-green in color, with a massive appearance and containing the following minerals: feldspar, peridots.
BD10	557,719	215,092	684	Medium-sized rock, grey-green in color, with a massive appearance and containing the following minerals: feldspar, peridots.
BD11	557,808	214,915	690	Medium-sized rock, grey-green in color, with a massive appearance and containing the following minerals: feldspar, peridots.
BD12	557,748	214,848	695	Medium-sized rock, grey-green in color, with a massive appearance and containing the following minerals: feldspar, peridots.
BD13	557,753	214,783	692	Medium-sized rock, grey-green in color, with a massive appearance and containing the following minerals: feldspar, peridots.

3.2. Petrographic Characteristics

Three petrographic facies were identified and are described below.

A. Dolerite Facies

The dolerite facies is represented by sample BD01, collected from a massive outcrop intersected by a quartz vein approximately 50 cm thick, striking N235˚ and dipping 78˚ NW (**Figure 5**).

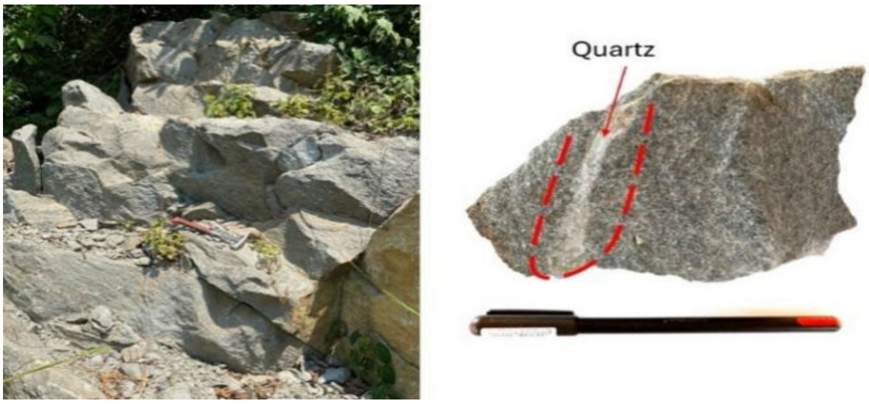

Figure 5. Outcrop view of the dolerite and quartz vein.

Macroscopically, the rock is greyish green, medium-grained, and massive. It consists predominantly of feldspar and quartz associated with dark ferromagnesian minerals. Disseminated iron sulphides are locally present, and the dolerite is cross-cut by a conspicuous milky quartz vein, indicating a later brittle-deformation event.

Under the polarizing microscope, the rock displays a typical doleritic (subophitic) texture characterized by elongated plagioclase laths intergrown with pyroxene. Pyroxene occurs as brown crystals in plane-polarized light and green crystals under crossed polars. Plagioclase is colourless in plane-polarized light and displays characteristic grey interference colours under crossed polars. Minor opaque minerals are also present. The observed mineral assemblage and characteristic doleritic texture confirm the classification of sample BD01 as dolerite (**Figure 6**).

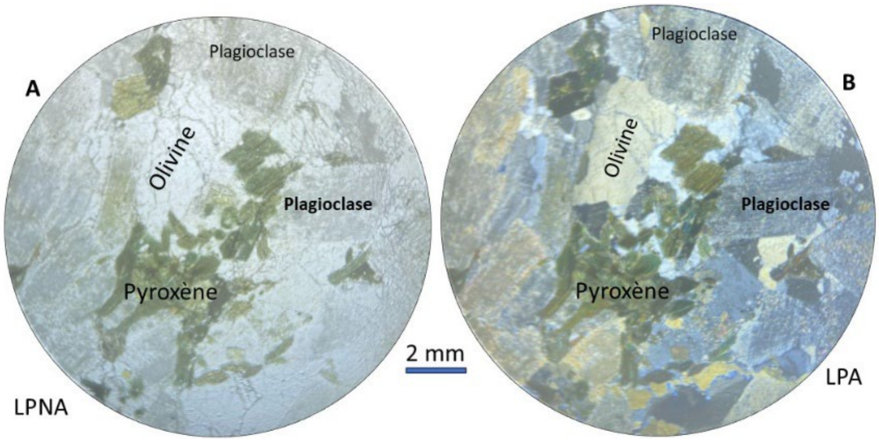

Figure 6. Microscopic observation of sample BD01 (dolerite).

B. Granite Facies

The granite facies is represented by sample BD02, collected from a massive granitoid outcrop exposed in the study area (**Figure 7**). Macroscopically, the rock is grey, medium-grained, and exhibits a typical granular texture. Its principal mineral constituents are quartz, orthoclase, muscovite, and biotite, which are uniformly distributed throughout the rock.

Figure 7. Outcrop view of the granite.

Microscopic examination reveals a holocrystalline granular texture composed of medium-sized interlocking crystals. Quartz occurs as anhedral, colourless grains in plane-polarized light and displays first-order grey interference colours under crossed polars. Orthoclase is abundant and is readily identified by its characteristic Carlsbad twinning, whereas albite exhibits well-developed polysynthetic twinning. Muscovite occurs as colourless flakes with moderate birefringence, while biotite occurs as brown pleochroic crystals. Minor opaque Fe-Ti oxides and disseminated iron sulphides are locally observed. This mineralogical assemblage and texture are consistent with the identification of sample BD02 as granite (Figure 8).

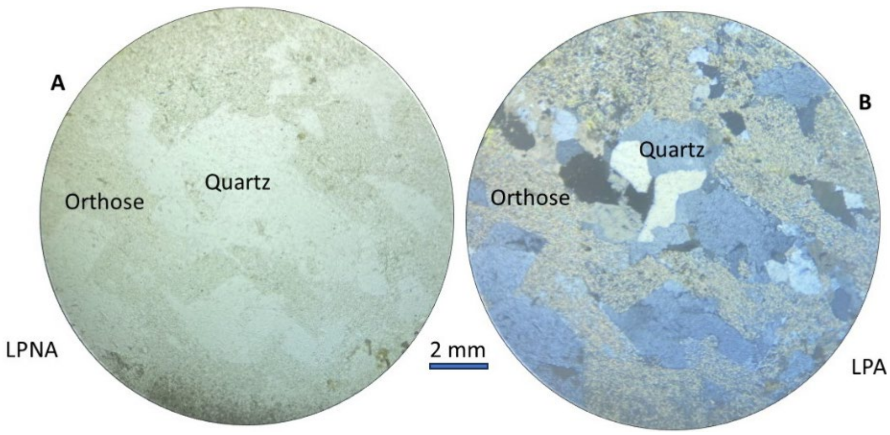

Figure 8. Microscopic observation of sample BD02 (granite).

C. Banded Iron Formation (BIF) Facies

The banded iron formation (BIF) facies is represented by sample BD06, collected from a foliated outcrop showing alternating iron-rich and silica-rich bands (Figure 9). Macroscopically, the rock is greyish brown to dark grey and displays a well-developed foliation striking N273˚ and dipping 32˚. The principal minerals identified in hand specimen are hematite, magnetite, and quartz, which define the characteristic banded appearance of the rock.

Figure 9. Macroscopic observation of BIF.

Microscopic examination shows a well-developed banded texture consisting of alternating quartz-rich and iron-rich layers. The siliceous bands are composed predominantly of anhedral quartz grains that are colourless in plane-polarized light and display first-order grey interference colours under crossed polars. The ferruginous bands contain abundant opaque iron oxides, mainly hematite and magnetite, disseminated within the siliceous matrix. This regular alternation of silica-rich and iron-rich layers is characteristic of banded iron formations and confirms the identification of sample BD06 as BIF (Figure 10).

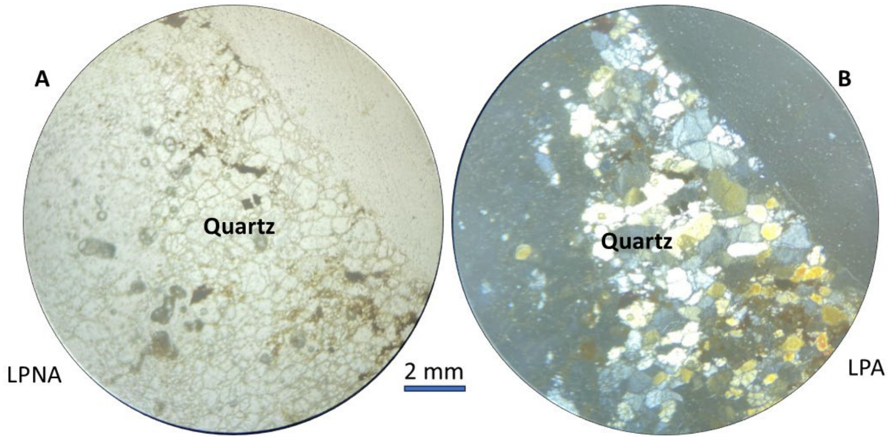

Figure 10. Microscopic observation of sample BD06 (BIF).

3.3. Geochemical and Metallogenic Analyses

3.3.1. Geochemical Analysis

Three representative samples (BD05, BD06, and BD01b) were analysed for major oxides and trace elements by energy-dispersive X-ray fluorescence (ED-XRF) at the Regional Nuclear Research Center of Kinshasa (CREN-K), Democratic Republic of the Congo.

Approximately 5 g of powdered sample was mixed with 1 g of Fluxana binder, homogenized, and pressed into pellets using a hydraulic press before analysis. Major oxides are reported in wt.%, whereas trace elements are expressed in ppm.

The analyses were performed using an XEPOS III ED-XRF spectrometer following the manufacturer's analytical protocol. Instrument calibration was achieved using certified reference materials (ISE2232, ISE1042, IPE1314, IPE2444, and PT2304 SOIL). Analytical precision and accuracy were evaluated using the laboratory quality-control procedure, and the results are reported with 95% confidence intervals.

The analytical results for major oxides and trace elements are presented in Table 2.

Table 2. Major-oxide (wt.%) and trace element (ppm) compositions of the investigated samples.

Parameter	Unit	BD05 (BIF)	BD06 (BIF)	BD01b (Quartz vein)
Major Oxides	wt.%			

Continued

SiO_2	wt.%	7.20	45.50	71.80
Al_2O_3	wt.%	38.60	12.50	7.40
Fe_2O_3	wt.%	15.80	22.30	6.10
MgO	wt.%	6.10	3.60	2.80
CaO	wt.%	9.40	5.10	3.20
Na_2O	wt.%	3.20	1.80	1.40
K_2O	wt.%	5.80	2.10	1.90
TiO_2	wt.%	1.10	0.80	0.70
P_2O_5	wt.%	0.35	0.22	0.18
MnO	wt.%	0.25	0.15	0.12
LOI	wt.%	11.70	5.50	4.20
Trace Elements	ppm			
Cr	ppm	0.75	0.75	243.70
Co	ppm	1.95	-	-
Ni	ppm	4.80	-	23.00
Cu	ppm	-	-	193.60
Zn	ppm	69.70	121.00	135.30
As	ppm	24.40	64.80	-
Rb	ppm	10.80	29.20	27.40
Nb	ppm	5.10	1.20	-
Sn	ppm	47.10	31.60	17.20
Sb	ppm	71.00	50.00	28.40
Ta	ppm	0.60	-	0.60
Pb	ppm	-	-	0.60

3.3.2. Metallogenic Analysis

Polished sections were prepared from the mineralized samples BD05, BD06, and BD01b to characterize opaque mineral assemblages under reflected-light microscopy. These samples were selected because they are representative of the main lithologies and contain visible metallic minerals observed in the field.

Sample BD06 (BIF). Macroscopically, the rock is characterized by alternating millimetre-scale silica-rich and iron-rich bands. Reflected-light microscopy reveals abundant hematite occurring as irregular patches disseminated within a quartz-rich gangue. The hematite grains are distributed throughout the rock, confirming the ferruginous nature of the BIF (Figure 11 and Figure 12).

Figure 11. BIF sample BD06.

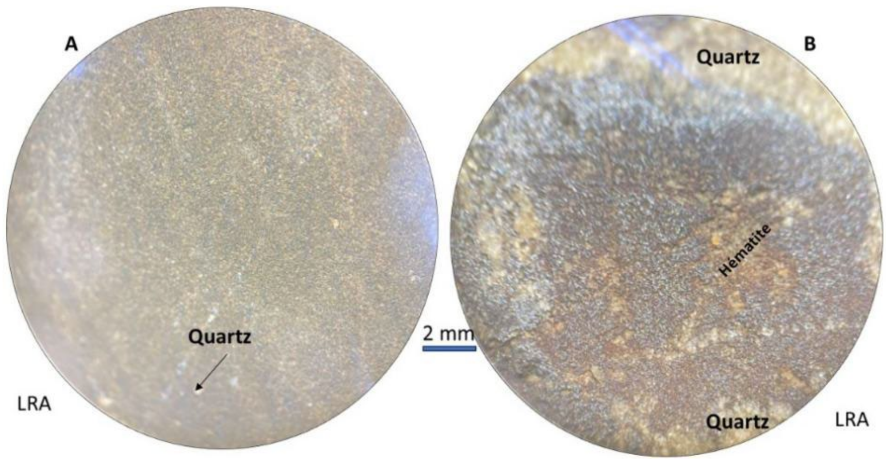

Figure 12. BIF sample BD06 under reflected light: (A) Reflected light; (B) Reflected light.

Sample BD05 (BIF). In hand specimen, the rock has a massive grey-black appearance with iron-rich bands alternating with silica-rich layers. Microscopic observations indicate that the gangue consists predominantly of quartz, within which hematite occurs as fine disseminated grains and thin laminae (Figure 13 and Figure 14).

Figure 13. BIF sample BD05.

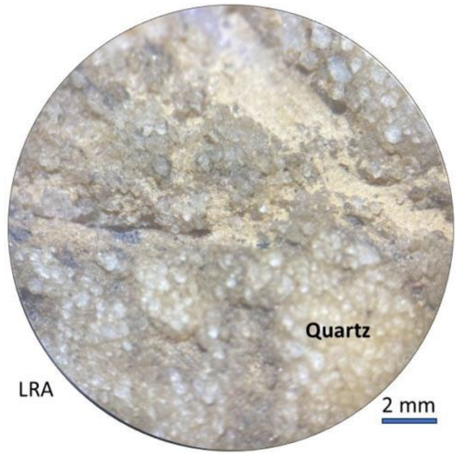

Figure 14. BIF sample BD05 under reflected light.

Sample BD01b (quartz vein). The sample consists of a milky quartz vein containing disseminated bright-yellow sulphide grains identified as pyrite. Under reflected light, pyrite occurs as euhedral to subhedral crystals embedded in a quartz matrix, indicating sulphide mineralization associated with the quartz vein (Figure 15 and Figure 16).

Figure 15. Quartz vein, sample BD01b.

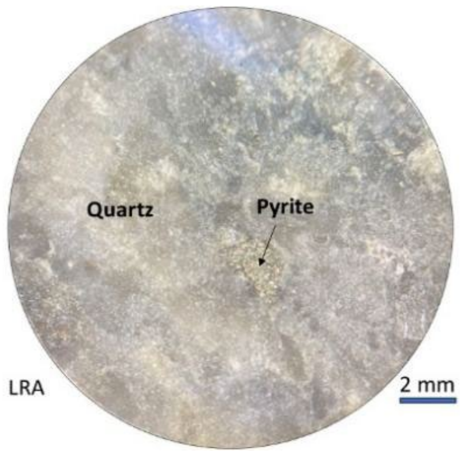

Figure 16. Quartz vein, sample BD01b, under reflected light.

4. Discussion

4.1. Petrographic Implications

The petrographic investigation identified three principal lithological facies in the Lassa area: dolerite, granite, and banded iron formation. These lithologies reflect distinct geological processes that contributed to the evolution of the Kibalian greenstone belt. Their coexistence represents an association of intrusive igneous rocks and chemical sedimentary formations, a characteristic feature of Precambrian greenstone terranes (Cahen & Lepersonne, 1967; Lavreau, 1982).

The dolerite is characterized by a typical doleritic texture composed of plagioclase, pyroxene, and olivine, indicating crystallization from a mafic magma at shallow to intermediate crustal levels. Quartz veins cutting the dolerite demonstrate that brittle fracturing and subsequent hydrothermal-fluid circulation occurred after magma emplacement. Such structural relationships are commonly reported in the Kibalian terrane and other Archean greenstone belts (Lavreau & Ledent, 1975; Mbo et al., 2024).

The granite displays a holocrystalline granular texture dominated by quartz and feldspars associated with muscovite and biotite. This mineral assemblage is consistent with the slow crystallization of felsic magma at depth and reflects the widespread granitoid intrusions that characterize the Kibalian basement (Cahen & Lepersonne, 1967; Lavreau, 1982).

The BIF is distinguished by alternating silica-rich and iron-rich bands composed mainly of quartz, hematite, and magnetite. Such banding is typical of Precambrian chemical sedimentary rocks and reflects successive precipitation of silica and iron under fluctuating physicochemical conditions in ancient marine environments (Klein, 2005; Morris, 1985).

Overall, the petrographic characteristics confirm that the Lassa area preserves the typical lithological association of the Kibalian greenstone belt, where granitoids, mafic intrusions, and banded iron formations provide a favourable geological framework for subsequent hydrothermal activity and associated mineralization. These mineral assemblages are consistent with those described in other Precambrian terranes (Nicollet, 2010).

4.2. Geochemical Implications

The geochemical compositions of the investigated samples reveal marked variations that reflect contrasting lithologies and the influence of hydrothermal processes. Major-oxide and trace-element distributions are consistent with the petrographic observations and provide insight into the geological evolution of the Lassa area. Major-element geochemistry is widely used to evaluate rock composition, alteration processes, and crustal evolution (Taylor & McLennan, 1985).

The BIF sample BD05 is characterized by very low SiO_2 (7.20 wt.%), high Al_2O_3 (38.60 wt.%), Fe_2O_3 (15.80 wt.%), and relatively high loss on ignition (LOI = 11.70 wt.%). These features indicate intense weathering and secondary alteration that probably modified the primary composition of the iron formation. The elevated

LOI further suggests hydration and supergene-alteration processes (Rollinson, 1993; Morris, 1985). The unusually high Al_2O_3 content of BD05 may reflect intense weathering, clay-mineral enrichment, or localized hydrothermal alteration. Consequently, this composition is interpreted as representing an altered BIF rather than its original primary geochemical signature.

Compared with BD05, sample BD06 contains higher SiO_2 (45.50 wt.%) and Fe_2O_3 (22.30 wt.%), together with lower Al_2O_3 (12.50 wt.%). This composition is consistent with a silica-rich banded iron formation in which iron oxides and quartz are the dominant mineral phases. The relatively elevated MnO content (0.15 wt.%) may reflect interaction with Mn-bearing hydrothermal fluids and is consistent with hydrothermal alteration associated with iron enrichment (Klein, 2005; Huston et al., 2011).

The quartz-vein sample BD01b is distinguished by its high SiO_2 content (71.80 wt.%), confirming its predominantly siliceous composition. Its relatively low Fe_2O_3 content (6.10 wt.%) is consistent with petrographic observations of a quartz-rich vein containing only minor sulphide minerals. Nevertheless, enrichment in Cr (243.70 ppm), Cu (193.60 ppm), and Zn (135.30 ppm), together with the occurrence of disseminated pyrite observed under reflected light, indicates that hydrothermal fluids capable of transporting metallic elements affected the quartz vein (Groves et al., 1998; Robb, 2005).

Overall, the geochemical data indicate that the BIFs record iron enrichment accompanied by variable silicification. Silica enrichment in banded iron formations is commonly associated with hydrothermal remobilization and silica precipitation during post-depositional alteration (Klein, 2005), whereas the quartz vein records intense silicification associated with hydrothermal sulphide mineralization. These characteristics support the interpretation that the Lassa area provides a favourable geological setting for further exploration of hydrothermal mineral systems (Goldfarb et al., 2005; Groves et al., 1998). Comparable silica-rich hydrothermal alteration has also been reported from Proterozoic successions of Central Africa (Poidevin, 1996).

4.3. Metallogenic Implications

The petrographic, geochemical, and mineragraphic data indicate that the Lassa area has geological characteristics favourable for hydrothermal mineralization. Quartz veins cutting the host rocks, together with disseminated pyrite observed in sample BD01b, suggest that hydrothermal fluids circulated through fracture systems after emplacement of the host lithologies. Such structural and mineralogical associations are typical of hydrothermal systems developed within Precambrian greenstone belts (Groves et al., 1998; Goldfarb et al., 2005). Similar structural controls have been described for the Kilo-Moto gold district. The relationship between regional structures and hydrothermal mineralization has long been recognized in the Kilo area (Woodtli, 1961).

The BIF samples contain abundant hematite and magnetite associated with quartz-rich layers. These iron-rich formations may have acted as chemically reactive host rocks during hydrothermal-fluid circulation, promoting sulphide precipitation where suitable structural and physicochemical conditions existed. Similar relationships between BIFs and hydrothermal mineralization have been documented in several Archean greenstone belts worldwide (Klein, 2005; Robb, 2005).

The quartz-vein sample is characterized by a silica-rich composition and disseminated pyrite associated with Cr, Cu, and Zn enrichment. Although these features indicate hydrothermal activity, they do not by themselves demonstrate the presence of an economic gold deposit because no direct gold analyses were conducted in this study. Further investigations, including Au assays, sulphide geochemistry, fluid-inclusion studies, and stable-isotope analyses, are required to evaluate the origin and economic significance of the mineralization (Groves et al., 1998; Goldfarb et al., 2005).

Overall, the integration of petrographic, geochemical, and mineragraphic evidence suggests that the Lassa area is a promising target for future mineral exploration. Nevertheless, the present study should be regarded as a preliminary geological assessment, and further multidisciplinary investigations are required to confirm the extent and economic potential of the hydrothermal mineralization.

5. Conclusion

This study provides new petrographic, geochemical, and mineragraphic data on the Kibalian formations exposed in the Lassa area, Haut-Uélé Province, northeastern Democratic Republic of the Congo. Geological field investigations combined with laboratory analyses identified three principal lithological facies: dolerite, granite, and banded iron formation (BIF). These lithologies record the magmatic, sedimentary, and hydrothermal processes that contributed to the geological evolution of the Kibalian greenstone belt.

Petrographic observations show that the dolerite is composed mainly of plagioclase, pyroxene, and olivine, whereas the granite consists predominantly of quartz, feldspars, muscovite, and biotite. The BIF is characterized by alternating silica-rich and iron-rich bands composed principally of quartz, hematite, and magnetite. These mineralogical assemblages are consistent with lithological characteristics previously reported for the Kibalian terrane.

Geochemical analyses highlight marked compositional differences among the investigated lithologies. The quartz vein has a silica-rich composition associated with disseminated pyrite and trace-element enrichment, whereas the BIF samples exhibit variable degrees of iron enrichment and silicification. These features indicate hydrothermal alteration and fluid circulation within the study area. However, the present data do not constitute direct evidence of economic gold mineralization because no gold assays were performed.

Overall, the integration of field observations, petrographic, geochemical, and metallographic data indicates that the Lassa area represents a favourable geological environment for hydrothermal mineralization within the Kibalian greenstone belt. Future investigations should include direct gold analyses, sulphide geochemistry, fluid-inclusion studies, isotopic investigations, and structural analyses to better constrain the origin, evolution, and economic significance of the mineralization.

Author Contributions

Conceptualization, Blaise Mutombo Kabulu; methodology, Blaise Mutombo Kabulu, Richard Logro Sapa, Jean-Luc Albini Tshupa and Jean-Paul Bakajika Kabongo; investigation, Blaise Mutombo Kabulu, Jean-Luc Albini Tshupa, Junior Lele Mambwiya, and Joseph Lelo Nkenge; formal analysis, Blaise Mutombo Kabulu, Richard Logro Sapa, and Adalbert Jule Makutu Ma Ngwayaya; data curation, Divine Biaya Tshiala and Herman Sadimoke Ibingo; writing—original draft preparation, Blaise Mutombo Kabulu; writing—review and editing, Blaise Mutombo Kabulu, Richard Logro Sapa, Jean-Luc Albini Tsupa, Jean-Paul Bakajika Kabongo, Junior Lele Mambwiya, Joseph Lelo Nkenge, Adalbert Jule Makutu Ma Ngwayaya, and Giresse Kabemba Kalonji; software, Blaise Mutombo Kabulu and Richard Logro Sapa; visualization, Blaise Mutombo Kabulu and Jean-Luc Albini Tshupa; supervision, Giresse Kabemba Kalonji and Adalbert Jule Makutu Ma Ngwayaya; project administration, Blaise Mutombo Kabulu. All authors have read and agreed to the published version of the manuscript.

Conflicts of Interest

The authors declare no conflicts of interest regarding the publication of this paper.

References

Cahen, L., & Lepersonne, J. (1956). *Congo belge. Lexique stratigraphique international, Volume IV, Afrique, Fascicule 7a* (121 p.). Centre National de la Recherche Scientifique.

Cahen, L., & Lepersonne, J. (1967). The Precambrian of the Congo, Rwanda and Burundi. In K. Rankama (Ed.), *The Precambrian* (Vol. 3, pp. 143-290). Interscience Publishers.

Cahen, L., Snelling, N. J., Delhal, J., Vail, J. R., Bonhomme, M., & Ledent, D. (1984). *The Geochronology and Evolution of Africa* (512 p.). Clarendon Press.

de Dorlodot, L., & Mathieu, F. F. (1928). Itinéraire géologique Zobia-Poko. *Annales de la Société Géologique de Belgique, Publications Relatives au Congo Belge et aux Régions Voisines, 51,* C95-C100.

de Dorlodot, L., & Mathieu, F. F. (1929). Itinéraire Géologique Duru-Gombari-Arebi. *Annales de la Société Géologique de Belgique, Publications Relatives au Congo Belge et aux Régions Voisines, 52,* C159-C166.

de Dorlodot, L., & Mathieu, F. F. (1931). Reconnaissance géologique du bassin de la haute Duru. *Annales de la Société Géologique de Belgique, Publications Relatives au Congo Belge et aux Régions Voisines, 54,* C107-C120.

Duhoux, P. V. (1950). Petrogenesis and Metallogeny of the Kilo-Moto Mining Area. *Annales de la Société Géologique de Belgique, 73,* 171-243.

Geological Survey of Zaire (1974). *Explanatory Note for the Map of Mineral Deposits in Zaire*. Department of Mines, Directorate of Geology.

Goldfarb, R. J., Baker, T., Dubé, B., Groves, D. I., Hart, C. J. R., & Gosselin, P. (2005).

Distribution, Character, and Genesis of Gold Deposits in Metamorphic Terran. In J. W. Hedenquist et al. (Eds.), *One Hundredth Anniversary Volume* (pp. 407-450). Society of Economic Geologists. https://doi.org/10.5382/av100.14

Groves, D. I., Goldfarb, R. J., Gebre-Mariam, M., Hagemann, S. G., & Robert, F. (1998). Orogenic Gold Deposits: A Proposed Classification in the Context of Their Crustal Distribution and Relationship to Other Gold Deposit Types. *Ore Geology Reviews, 13,* 7-27. https://doi.org/10.1016/s0169-1368(97)00012-7

Huston, D. L., Pehrsson, S., Eglington, B. M., & Zaw, K. (2011). The Geology and Metallogeny of Volcanic-Hosted Massive Sulfide Deposits: Variations through Geologic Time and with Tectonic Setting. *Economic Geology, 105,* 571-591. https://doi.org/10.2113/gsecongeo.105.3.571

Klein, C. (2005). Some Precambrian Banded Iron-Formations (BIFs) from around the World: Their Age, Geologic Setting, Mineralogy, Metamorphism, Geochemistry, and Origins. *American Mineralogist, 90,* 1473-1499. https://doi.org/10.2138/am.2005.1871

Lavreau, J. (1982). *Geological Study of Upper Zaire. Genesis and Evolution of an Archean Lithospheric Segment* (p. 109). Royal Museum for Central Africa-Tervuren, Belgium Annals-Series, No. 88; Geological Sciences, No. 88.

Lavreau, J., & Ledent, D. (1975). Establishment of the Geochronological Framework of the Kibalian (Zaire). *Annales de la Société Géologique de Belgique, 98,* 197-212.

Legraye, M. (1940). *Grands traits de la géologie et de la minéralisation aurifère des régions de Kilo et de Moto (Congo belge).* https://www.kaowarsom.be/documents/MEMOIRES_VERHANDELINGEN/Sciences_techniques/Tec.Sc.(IRCB)_T.II,3_LEGRAYE,%20M._Grands%20traits%20de%20la%20g%C3%A9ologie%20et%20de%20la%20min%C3%A9ralisation%20aurif%C3%A8re%20des%20r%C3%A9gions%20de%20Kilo%20et%20de%20Moto%20(Congo%20belge)_1940.PDF

Lepersonne, J. (1974). *Explanatory Note for the Geological Map of Zaire at 1:2000000, Department of Mines, Directorate of Geology* (p. 67). Royal Museum of Central Africa and CRGM.

Mbo, L. M., Nkula, V. K., & Tienge, A. O. (2024). Analyses pétrographique et géochimique des itabirites des Monts Zatua dans la Province de Haut-Uélé en République Démocratique du Congo. *Revue Africaine d'Environnement et d'Agriculture, 7,* 53-66. https://doi.org/10.4314/rafea.v7i2.7

Morris, R. C. (1985). Genesis of Iron Ore in Banded Iron-Formation by Supergene and Supergene-Metamorphic Processes—A Conceptual Model. In *Regional Studies and Specific Deposits* (pp. 73-235). Elsevier. https://doi.org/10.1016/b978-0-444-42497-6.50006-0

Nicollet, C. (2010). Metamorphism and Geodynamics (p. 288). Dunod.

Poidevin, J. L. (1996). The Upper Proterozoic of the Republic: A Proximal Segment of Upper Proterozoic Age Carbonate Ramp in the North of the Central African Craton (Southeast of the Central African Republic). *Journal of African Earth Sciences, 23,* 257-262.

Robb, L. (2005). *Introduction to Ore-Forming Processes*. Blackwell Publishing.

Rollinson, H. R. (1993). *Using Geochemical Data: Evaluation, Presentation, and Inter-Pretation*. Longman Scientific & Technical.

Taylor, S. R., & McLennan, S. M. (1985). *The Continental Crust: Its Composition and Evolution*. Blackwell Scientific Publications.

Verbeek, T. (1970). *Geology and Lithology of the Lindian (Upper Precambrian of the North of the Democratic Republic of Congo)* (309 p.). Ed. MRAC.

Woodtli, R. (1961). Relationships of General Structure to Gold Mineralization in the Kilo Area (Central Africa). *Economic Geology, 56,* 584-591. https://doi.org/10.2113/gsecongeo.56.3.584